

Compress & Align: Curating Image-Text Data with Human Knowledge

Lei Zhang^{1,2*} Fangxun Shu^{2*} Sucheng Ren³ Bingchen Zhao⁴
 Hao Jiang^{2†} Cihang Xie^{5†}

¹Zhejiang University ²Alibaba Group ³Johns Hopkins University
⁴University of Edinburgh ⁵University of California, Santa Cruz

Abstract

The massive growth of image-text data through web crawling inherently presents the challenge of variability in data quality. This paper introduces a novel algorithm, rooted in human knowledge, to compress this vast corpus of web-crawled image-text datasets to a compact and high-quality form. Our method unfolds in three major steps. First, we collect an image-text dataset, wherein each image is associated with multiple captions sourced from diverse origins. Then, to systemically capture human preferences regarding the best caption paired with each image, we establish a comprehensive set of both subjective and objective criteria for critically guiding the alignment assessment from labelers. Lastly, we train a reward model on the annotated dataset to internalize the nuanced human understanding of image-text alignment. The resulting reward model thus can act as a human-like referee to filter misaligned/low-quality image-text pairs.

Extensive experiments demonstrate that we are able to secure (or even improve) model performance by compressing the image-text datasets up to $\sim 90\%$. An impressive example is that, by aggressively reducing the total training sample from 130M to 15.5M (e.g., $\sim 9\times$ smaller), our BLIP-B/16 models still consistently show superior performance compared with the full-size-dataset counterpart on image-text retrieval (Flickr30K, COCO) by $\sim 2.5\%$ in Recall@1, and on image-captioning (Nocaps, COCO) by $\sim 10.0\%$ in CIDEr and $\sim 2.7\%$ in SPICE.

1. Introduction

The rapid progress in vision-language foundation models [2, 5, 11, 26, 29, 35] has been largely driven by the growing availability of image-text pairs, experiencing a massive escalation from datasets comprising a few million samples, such as COCO [20], CC3M [35] and CC12M [5], to those encompassing billions, exemplified by YFCC-100M [37],

*Equal contribution.

†Corresponding author.

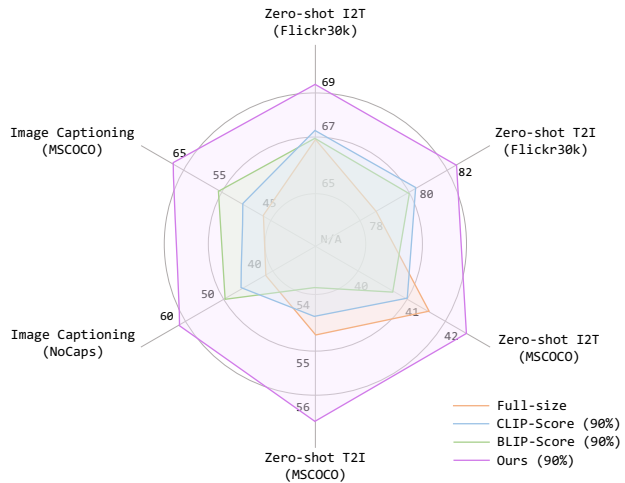


Figure 1. Our method outperforms full-size training dataset on various downstream tasks with BLIP-B/16. This training set consists of CC3M, CC12M, and a subset of LAION-400M. We reduce the training sample size from 130M to 15.5M (i.e. $\sim 9\times$ smaller).

LAION-400M [32], and LAION-5B [33]. Typically, to facilitate the large-scale collection of such data, web crawling is applied with simple filtering mechanisms in place. While this collection pipeline ensures a rich diversity of data, it inadvertently introduces significant variability in data quality, presenting new challenges for learning at scale.

A popular strategy for mitigating this challenge is data filtering. Recent literature illustrates various methodologies where models are designed to assess the alignments between images and their corresponding textual descriptions, selectively retaining only those pairs that meet predefined standards [38, 40]. However, a fundamental concern associated with this line of work is that the filtering models are typically built upon the original, uncurated datasets, which are inherently noisy, as illustrated in the upper part of Fig. 2. This noise can possibly propagate biases and misalignments into filtered datasets, potentially impinging upon the top-line performance for subsequent models trained on such data. Moreover, the intrinsic cognitive discrepancies between human and machine perception, as studied in recent

works [17, 24, 31], suggest that machine-based assessments alone may not sufficiently encapsulate the quality standards set by human judgment.

Intriguingly, recent advancements in language models [3, 15, 22, 25, 44] have demonstrated that Reinforcement Learning from Human Feedback (RLHF) [6, 36] can effectively incorporate human preferences as a reward signal, markedly aligning the model with human intentions. A key component here is the reward model, which is trained to approximate the often complex and nuanced human evaluations of desired behavior. By integrating human feedback directly into the training loop, models can develop a more profound understanding of complex domains of human knowledge. Inspired by these advancements, this paper seeks a human-centric approach to the curation of image-text pairings, aiming to improve data quality through a filtration process intrinsically attuned to the subtleties of human cognition and evaluative criteria, as illustrated in the bottom part of Fig. 2.

An overview of our data filtering pipeline, which is grounded in human knowledge, is illustrated in Fig. 3. Specifically, our first step is to collect a dataset with 10,000 images, each paired with a variety of captions. Then, human preferences are collected on ranking the alignment between different captions to their corresponding images, applying a set of criteria that captures both objective aspects, such as accuracy and completeness, and subjective aspects, such as vividness and contextual relevance. In the final stage, we train a reward model on the annotated dataset, aiming to predict the human preference for captions. The resulting reward model is expected to function as a human-like referee that can transfer human knowledge to identify and filter the misaligned and low-quality image-text pairs for enhancing the overall dataset quality.

Extensive experiments are provided on demonstrating that we can successfully compress large-scale and noisy image-text datasets to compact and well-aligned forms. For example, as shown in Fig. 1, by compressing the training dataset, consisting of CC3M [35], CC12M [5], and a portion of the LAION-400M dataset [32], from 130M to 15.5M, BLIP-B/16 achieves a highly competitive 82.4% zero-shot text recall@1 (Flickr30K [28]) and 61.7% zero-shot CIDEr (Nocaps [1] val set). This performance stands in stark contrast to the counterpart trained on the original 130M dataset, which attains 78.6% on text recall@1 and 0.0 on CIDEr. Additionally, our method exhibits a good generalization to different vision-language models — with CLIP-B/16 model, we not only reduce the dataset by 50% but also impressively achieve 2.6% and 2.0% improvements on text and image recall@1 (Flickr30K).

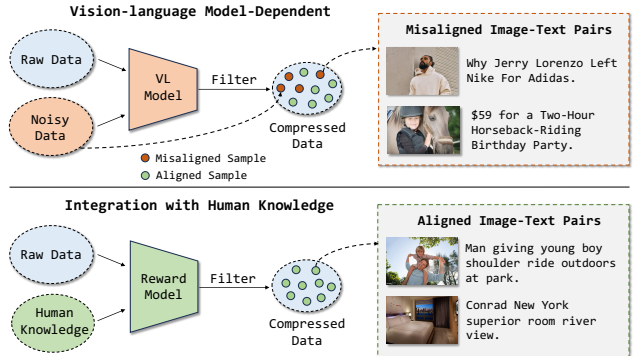


Figure 2. The upper side demonstrates the pipeline of filtering method based on feature similarity. The bottom side demonstrates the pipeline of our method integrated with human knowledge

2. Related Work

Learning from human knowledge. The integration of human knowledge is becoming progressively instrumental in aligning model behavior with human intent [3, 15, 17, 22, 39, 41, 43, 44]. The key part is to train a reward model [21] to directly capture human preferences regarding the outputs generated by the model. Recent works propose to utilize reinforcement learning [34] to finetune the language models [25] and diffusion models [17, 41, 43] with the signal of reward model. However, few studies focus on utilizing human knowledge to directly improve dataset quality. This work pioneers the exploration of integrating human knowledge with image-text data to relieve the visual and textual misalignment in large-scale image-text datasets.

Vision-language data. Data is of central importance to the success of vision-language pre-training at scale [2, 11, 29]. Early efforts in dataset collection often employ simple but vague cleaning strategies [5, 35, 37]. Recently it has turned to focusing on visual and textual alignment to intricately filter misaligned image-text pairs, *e.g.*, LAION-400M [32] utilized similarity scores of pre-trained CLIP model [29] to filter low-quality image-text pairs. Further advancements include CiT [40], which trains models with dynamic training data on the fly, and TL;DR [38], which learns a trainable codebook separately by image feature extraction and language modeling. However, these data-filtering models are typically built upon noisy datasets, therefore potentially being less effective in filtering data. Differently, in this work, we directly introduce human preference into data filtering for evaluating dataset quality.

3. Method

To improve image-text datasets with human knowledge, we follow the steps shown in Fig. 3. We first generate a set of diverse captions for a given set of images, subsequently soliciting human assessments to determine the degree of alignment between each image and its associated captions.

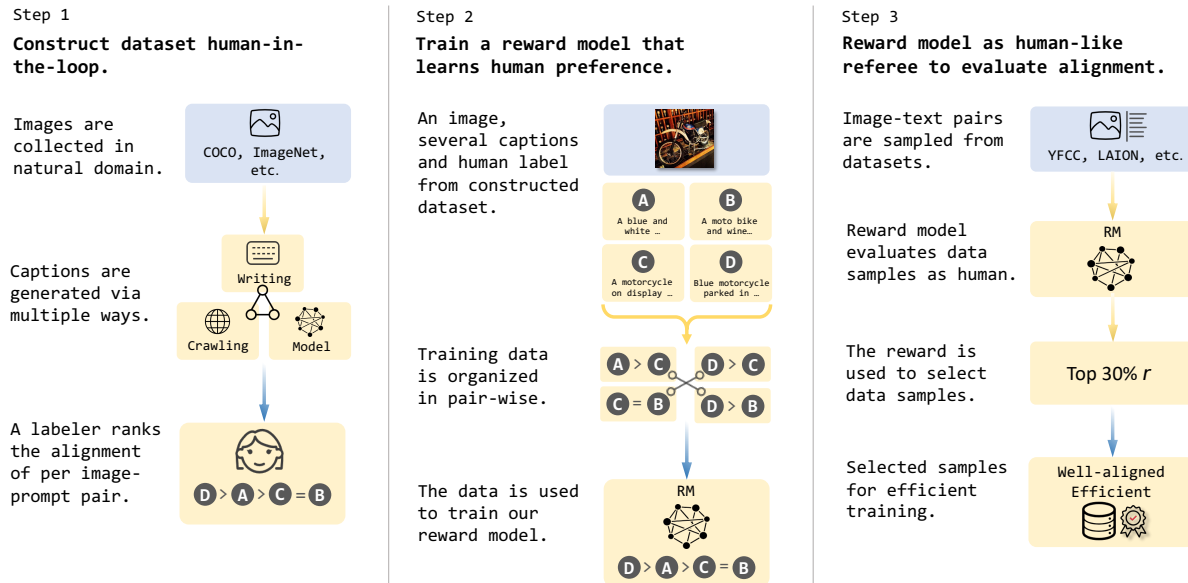


Figure 3. A diagram illustrating the three steps of our method. We first curate an image-text dataset to collect human knowledge on alignment in Stage 1. Then we train a reward model to predict human preference in Stage 2. The reward model is functioned as a human-like referee to filter misaligned image-text pairs in Stage 3. *The style of this figure is inspired by Figure 2. in InstructionGPT [25].

This phase involves a comprehensive scoring process by labelers to evaluate the quality of image-caption alignment, as detailed in Sec. 3.1. Next, we train a reward model to emulate human evaluative feedback, taking an image and a corresponding caption as inputs, an approach elaborated upon in Sec. 3.2. The resulting reward model is expected to function as a human-like referee to improve image-text datasets (see Sec. 3.3).

3.1. Human Knowledge Collection

We construct a systematic pipeline to build an image-text dataset enriched with human feedback, as delineated in Step 1 of Fig. 3. This pipeline contains two integral components: the collection of image-caption data and the subsequent annotation of this data with human feedback provided by expert labelers. This built image-caption dataset is expected to be both well-aligned and diverse: on an individual level of image-text pair, the caption contains rich and useful visual information accurately reflecting the image’s content; on a population level of dataset, the distribution of captions is diverse preventing biases from a single source.

Image-Captions Collection. We utilize MSCOCO [20] as the basis to curate our new dataset, termed *COCO-HF*. To enrich the diversity of captions, we explore the following strategies:

- **MSCOCO Sampling.** Note that multiple text descriptions for one image are already available in the original MSCOCO dataset, *i.e.*, each image is associated with five distinct human-write text descriptions.
- **Model Rewriting.** We also employ various generative models, such as BLIP [18], BLIP-2 [19], and Instruct-

BLIP [7] to generate captions using images as inputs and prompts optionally.

- **Human Rewriting.** Additionally, we engage human annotators and task them with rewriting captions based on content depicted in the corresponding observed images.

With these three steps, we collect a dataset with 1,000 candidate images, each accompanied by 8 to 10 captions.

Human-Preference Annotations. We recruit well-trained human labelers to evaluate the alignment between generated captions and image content. To ensure annotation consistency, we instituted four precise guidelines that outline the criteria for alignment, with illustrative examples provided in Fig. 4:

- **Accuracy.** The caption should first accurately reflect the content of the corresponding image. The inaccurate captions include descriptions conflicted with the content of the image, fabrication not relying on corresponding images, *etc.*
- **Completeness.** The caption should contain the main visual objects in the image as completely as possible. It guarantees the caption acknowledges an abstract view of the whole image.
- **Vividness.** The caption should describe the details of the mentioned visual objects. The details here refer to the number, appearance, action, and status of the visual objects. The vivid captions provide individual status and relationships between different visual objects, which is a kind of comprehensive understanding of the image.
- **Context.** The caption should mention the context of the image, which is easily ignored. The context includes the background where the image occurs and the atmosphere

that the image conveys or implies. It contains complete observation and human understanding of the image.

These criteria collectively contribute to a multi-faceted annotation framework that captures both the objective denotations and the subjective connotations of image-text pair.

3.2. Reward Model Training

Inspired by InstructGPT [25], we propose to train a reward model to learn the human preference knowledge on COCO-HF dataset. This reward model is designed to capture the subtleties of human preferences, thereby serving as an automatic, yet human-like, arbiter for aligning image-text correspondences. (seen in Fig. 3 Step 2).

We transform the preference annotations as rankings and formulate the training of the reward model as a pairwise ranking problem. For each given image I in the COCO-HF dataset, we have $k \in [8, 10]$ textual captions ranked by human labelers, which are denoted as x_1, x_2, \dots, x_k . If x_i is better than x_j , we organize (I, x_i, x_j) as a comparison pair. This produces at most C_k^2 comparison pairs for each image. Then, we follow the Bradley-Terry model [4, 25] of preferences to define the pair-wise loss function as:

$$loss(\theta) = -\mathbb{E}_{(I, x_i, x_j) \sim \mathcal{D}_H} [\log(\sigma(f_\theta(I, x_i) - f_\theta(I, x_j)))] \quad (1)$$

where $f_\theta(I, x)$ is a scalar value of reward model f parameterized by θ for image I and caption x . σ is the sigmoid function. \mathcal{D}_H is COCO-HF dataset.

Implementation. Following [41], our reward model f_θ contains BLIP [18] as the backbone and score mapping layer based on MLPs. The backbone produces a multi-modal embedding of image and text features, and the score mapping layer maps the multi-modal embedding to a scalar as the reward score. When training the reward model, we freeze the parameters of the backbone BLIP and take the MLP part as trainable. The hyperparameter setup and training details of reward model training are provided in the supplementary material.

3.3. Dataset Compression

In order to compress large-scale datasets into compact and well-aligned ones, we utilize the reward model as a human-like referee to filter misaligned image-text pairs (Step 3 in Fig. 3).

Let $\mathcal{D} = \{(I^n, x^n)\}_{n=1}^N$ be the original image-text dataset. We utilize the reward model f_θ to evaluate the image-text alignment of each image-text pair (I^n, x^n) from the dataset \mathcal{D} . The reward score r_i is formulated as $r^n = f_\theta(I^n, x^n)$. Then, we obtain the set of reward scores $R_{\mathcal{D}}$ of the whole dataset \mathcal{D} , which can be expressed as $R_{\mathcal{D}} = \{r^1, r^2, \dots, r^N\}$. In order to compress the original dataset \mathcal{D} to a compact and well-aligned dataset $\hat{\mathcal{D}}$ with $k\%$ original amount, we consist $\hat{\mathcal{D}}$ of image-text pairs with top $k\%$

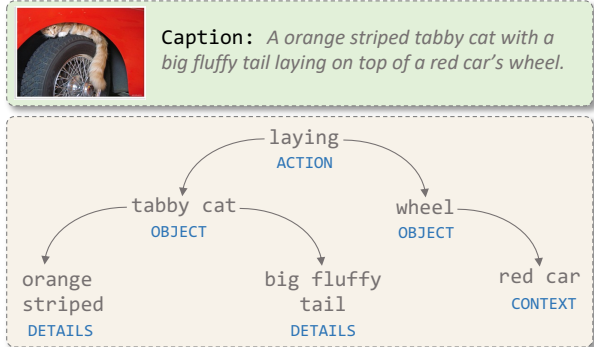


Figure 4. We provide an image-text pair as the example and employ our proposed criteria to evaluate the caption. The caption here is a high-quality exemplar since it satisfies all the requirements.

reward score in $R_{\mathcal{D}}$. We train the vision-language models with compressed dataset $\hat{\mathcal{D}}$ efficiently and evaluate on various downstream tasks.

4. Experiments

In this section, we provide extensive experiments to demonstrate the effectiveness of the proposed method in compressing vision-language data for better quality. The main results of RM are measured on human preference accuracy. The evaluation of data compression is presented next and organized as image-text retrieval tasks, image classification tasks, and image captioning tasks. We also present ablation studies, including data efficiency and vision-language model architecture.

4.1. Evaluation on Human Preferences

Alignment with Human. We first investigate the quality of our reward model and other image-text pair selection methods by evaluating its prediction in terms of human preference. We randomly choose 200 images from the MSCOCO dataset [20] and generate 8 to 10 captions for each image and human labelers rank the following Sec. 3.1 to curate a validation dataset. In addition to the proposed method, we consider the other two methods for comparison: CLIP Score, and BLIP Score. Our reward model is combined BLIP [18] model as the backbone with MLP to generate reward score. For each baseline, we consider different Vision Transformer backbone architectures including ViT-B/16 and ViT-L/16. We use these methods to select the best caption among the candidate captions for each image and evaluate the accuracy in accordance with human preference.

As shown in Fig. 5, our reward model achieves significant advantages over others. For example, while CLIP model achieves merely 40% accuracy, our method achieves over 70%. It suggests that existing vision-language models trained on noisy datasets are poor at aligning with human knowledge. The experiment results demonstrate that our re-

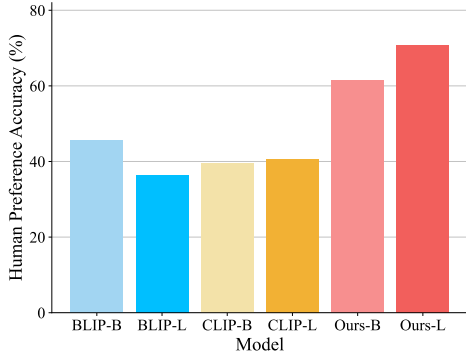


Figure 5. Accuracy of CLIP Score [29], BLIP Score [18], and our reward model with different ViT architectures on predicting preference of human labelers.

ward method effectively encodes human knowledge of visual and textual alignment. We adopt the reward model with a large backbone to filter misaligned image-text pairs in the following experiments.

Visualization. In order to demonstrate the performance of different filtering methods, we employ CLIP-Score, BLIP-Score, and our reward model with the large backbone to filter the Conceptual Captions 3M (CC3M) [35] dataset. We remain the image-text pairs in which the scores are ranked at the top 50% in the full-size dataset.

As shown in Fig. 6, we visualize the image-text pairs that are selected by our reward model but not selected by CLIP-Score and BLIP-Score. It demonstrates that our reward performs evident advantages over a fine-grained understanding of image and text contents, including position, appearance, and background, which is close to human perception.



Figure 6. We employ different methods to select the top 50% data from the CC3M dataset. The shown image-text pairs are selected by our method but excluded by CLIP Score and BLIP Score.

4.2. Evaluation on Data Selection

4.2.1 Training Setup

Datasets. We conduct experiments on three different image-text datasets at different scales: Conceptual Captions 3M (CC3M) [35], Conceptual Captions 12M (CC12M) [5], and LAION-400M [32]. The majority of our ablation studies are performed on the CC12M datasets. We compress the original datasets to 50% as default. Additionally, we explore different compression ratios in ablation studies.

Baselines. In addition to our method, we consider other three commonly-used baselines: random selection, CLIP Score [29], and BLIP Score [18]. The latter two methods target poorly aligned image-text pairs by using pre-trained CLIP models and BLIP models to rank the cosine similarity score between image and text embeddings. The CLIP and BLIP models are with a large ViT vision backbone.

Training Parameters. For our experiments on CC3M and CC12M, we utilize the BLIP [18] of ViT-B/16 [9] architecture. For LAION-400M, we use the ViT-L architecture and follow the exact training setup outlined in [18]. For CC3M dataset, we train the models with a batch size of 600 and the AdamW optimizer [14]. We set the batch size to 2, 880 for CC12M and LAION-400M datasets. The training epoch is 40 for CC3M and CC12M datasets and 5 for LAION-400M dataset, respectively. The learning rate is set to 3×10^{-3} , and weight decay is set to 0.1. The supplementary material contains a detailed breakdown of training parameters.

Evaluation Setup. We consider three downstream evaluation tasks for the trained BLIP models: image classification tasks, image-text retrieval tasks, and image captioning tasks. It is worth noting that we evaluate these tasks all in a zero-shot manner. In order to demonstrate the improvements in alignment of vision-language models, we do not fine-tune trained BLIP models to avoid bias from other datasets in fine-tuning.

4.2.2 Downstream Tasks

Zero-Shot Image-Text Retrieval. The task is to measure fine-grained world region alignment between images and texts. We evaluate the trained BLIP models on the two standard image-text retrieval benchmarks: MSCOCO [20] and Flickr30K [27]. Following previous work [13, 42], we use the Karpathy split [12] for the two benchmarks.

Tab. 1 shows the main results. Compared with the full-size CC12M dataset, our method improves text recall@1 from 81.0% to 81.6% with only 50% amount. This shows that we not only reduce data redundancy but also improve data quality. Furthermore, we observe consistent improvements in performance compared with other filtering methods when scaling up the dataset. The performance gap between our method and BLIP Score on Image Recall@1 is -0.4% on Flickr30K dataset and -0.1% on MSCOCO dataset, however, the gap enlarges to $+1.8\%$ and $+0.9\%$ when scaling from 3M to 12M. Compared with CLIP Score on CC12M dataset, we experience a 3.9% and 3.8% for text recall@1 on Flickr30K and MSCOCO dataset. It suggests that filtering with human knowledge effectively conveys the capability of a fine-grained understanding of the vision-language model.

Dataset	Method	#Samples	Text → Image						Image → Text					
			Flickr30K			MSCOCO			Flickr30K			MSCOCO		
			R@1	R@5	R@10	R@1	R@5	R@10	R@1	R@5	R@10	R@1	R@5	R@10
CC3M	-	2.82M	66.0	89.6	94.5	39.9	64.6	74.7	51.9	76.8	83.9	28.8	53.8	64.9
	Random	1.41M	57.7	84.2	91.0	30.7	56.7	68.7	44.4	71.3	79.5	24.7	48.4	59.6
	CLIP Score	1.41M	51.3	80.0	87.9	30.2	56.4	68.7	41.5	68.5	78.1	25.6	49.2	60.2
	BLIP Score	1.41M	61.4	87.8	93.2	36.8	62.8	74.2	49.7	75.2	82.9	28.7	53.7	64.8
	Ours	1.41M	64.2	87.5	92.5	37.4	63.9	74.6	49.3	74.8	82.8	28.6	53.2	64.1
CC12M	-	10.4M	81.0	95.6	97.4	53.5	77.2	85.7	65.0	87.4	92.1	39.2	65.0	74.8
	Random	5.20M	74.0	92.8	96.9	48.3	73.1	82.1	59.5	83.8	89.7	34.6	60.3	71.3
	CLIP Score	5.20M	77.7	95.2	97.4	49.7	75.4	83.8	62.1	83.9	89.6	36.0	61.9	72.5
	BLIP Score	5.20M	79.6	94.7	97.2	53.1	76.8	85.0	62.2	84.9	90.3	37.6	63.4	73.5
	Ours	5.20M	81.6	95.7	98.0	53.5	78.2	86.2	64.0	86.4	91.7	38.5	64.0	74.3

Table 1. Zero-shot image-text retrieval results on Flickr30K [27] and MSCOCO [20] datasets.

Dataset	Method	#Samples	MSCOCO				NoCaps			
			BLEU@4	CIDEr	METEOR	SPICE	Valid		Test	
							CIDEr	SPICE	CIDEr	SPICE
CC3M	-	2.82M	7.3	39.2	12.5	9.3	35.0	7.0	34.1	6.9
	Random	1.41M	7.5	37.8	12.7	9.2	34.6	6.9	33.5	7.0
	CLIP Score	1.41M	7.4	38.4	12.7	9.3	34.2	7.1	33.7	6.7
	BLIP Score	1.41M	8.5	42.4	13.5	9.9	38.1	7.3	37.1	7.3
	Ours	1.41M	12.9	48.7	16.4	11.9	46.1	8.6	44.5	8.6
CC12M	-	10.4M	11.4	42.7	14.2	10.3	38.6	7.7	36.1	7.6
	Random	5.20M	11.1	43.1	14.2	10.2	38.7	7.6	35.8	7.5
	CLIP Score	5.20M	13.8	49.6	16.5	11.8	46.1	8.7	43.6	8.7
	BLIP Score	5.20M	16.9	59.1	18.1	13.0	52.9	9.0	50.2	9.1
	Ours	5.20M	18.0	59.1	19.5	14.0	57.2	10.4	54.8	10.4

Table 2. Zero-shot image captioning results on MSCOCO [20] and NoCaps [1] datasets. Note that the models are not finetuned with CIDEr optimization on MSCOCO dataset.

Dataset	Method	#Samples	IN-1K	IN-A	IN-O
CC3M	-	2.82M	29.0	10.0	41.4
	Random	1.41M	27.5	9.5	37.8
	CLIP Score	1.41M	26.7	8.3	40.3
	BLIP Score	1.41M	29.6	9.2	41.7
	Ours	1.41M	29.7	11.0	42.0
CC12M	-	10.4M	48.8	18.1	62.1
	Random	5.20M	43.2	19.2	61.9
	CLIP Score	5.20M	51.3	21.0	66.2
	BLIP Score	5.20M	48.7	19.6	65.3
	Ours	5.20M	48.5	21.8	64.4

Table 3. Zero-shot image classification results on ImageNet-1K (IN-1K) [8], ImageNet-A (IN-A) [10], and ImageNet-O (IN-O).

Zero-shot Image Classification. We evaluate trained BLIP models on ImageNet with different distributions including ImageNet-1K [8], Imagenet-A [10], and ImageNet-O. We follow the exact setup in [29] and apply the same set of prompts used for label classnames to all the baselines.

Tab. 3 shows the main experiment results. We achieve improvement on full-size dataset with only 50% amount on CC3M dataset, for example improving from 29.7% to 29.0% on ImageNet-1K dataset, 11.0% to 10.0% on ImageNet-A dataset, 42.0% to 41.4% on ImageNet-O dataset. However, other filtering methods hurt performance

on most of datasets, for instance, CLIP Score hurts by 2.3% on ImageNet-1K, 1.7% on ImageNet-A, and 1.1% on ImageNet-O. However, the performance of our method becomes slightly worse when scaling up to the CC12M dataset. This indicates that the classification task heavily relies on visual diversity. Moreover, the prompts here are constructed by simply splicing classnames into a template, which cannot fully demonstrate the capability of textual and visual alignment.

Zero-shot Image Captioning. Additionally, we evaluate trained models on the image captioning task. The task is to generate a natural language caption for the given image. We consider two popular benchmarks: MSCOCO [20] and NoCaps [1]. Note that we do not evaluate the models finetuned on MSCOCO Karpathy split [12]. Since we investigate the alignment of models, finetuning tends to introduce biases.

Tab. 2 shows the main results. Compared with the full-size dataset, our method demonstrates a significant improvement with only 50% dataset, for instance from 38.6% to 57.2% on CIDEr, from 7.7% to 10.4% on NoCaps validation set. We observe consistent performance improvements when reducing the amount of dataset whatever filtering methods are applied. It suggests that misalignment seriously hurts the captioning performance. Our method

Dataset	Method	#Samples	Text \rightarrow Image						Image \rightarrow Text					
			Flickr30K			MSCOCO			Flickr30K			MSCOCO		
			R@1	R@5	R@10	R@1	R@5	R@10	R@1	R@5	R@10	R@1	R@5	R@10
CC+LAION	-	15M+115M	78.6	95.6	98.0	54.7	78.5	86.3	66.9	88.1	92.9	41.5	66.9	76.3
	CLIP Score	15M+8M	80.4	94.7	97.0	54.4	77.3	84.7	67.2	88.4	93.2	41.0	66.4	75.8
	BLIP Score	15M+8M	80.0	95.0	97.6	53.7	77.8	85.9	67.0	88.2	92.6	40.7	66.0	75.6
	Ours	15M+8M	82.4	96.4	98.8	56.7	79.9	87.2	69.6	89.3	93.6	42.6	68.0	76.9

Table 4. Performance of downstream tasks on BLIP of ViT-B/16 on image-text retrieval tasks. The CC dataset consists of the CC3M [35] and the CC12M [5] dataset. All the downstream tasks are evaluated in a zero-shot manner. Following BLIP [18], we filter the images whose short edge is smaller than 256 pixels from the original LAION-400M.

Dataset	Method	#Samples	MSCOCO				NoCaps			
			BLEU@4	CIDEr	METEOR	SPICE	Valid		Test	
							CIDEr	SPICE	CIDEr	SPICE
CC+LAION	-	15M+115M	9.1	46.7	14.0	10.3	41.6	7.6	40.0	7.5
	CLIP Score	7.5M+8M	11.5	50.2	15.0	11.1	45.5	8.2	43.4	8.1
	BLIP Score	7.5M+8M	13.2	55.4	16.3	12.0	51.5	8.5	49.0	8.5
	Ours	7.5M+8M	19.8	68.3	19.9	14.6	61.7	10.3	59.9	10.3

Table 5. Performance of downstream tasks on BLIP of ViT-B/16 on image captioning tasks. The CC dataset consists of the CC3M [35] and the CC12M [5] dataset. All the downstream tasks are evaluated in a zero-shot manner.

significantly outperforms other methods. We experience a +4.3% gap on CIDEr compared with BLIP Score and a +11.1% gap compared with CLIP Score, further suggesting that our efforts to examine the vividness of textual captions empower models with a powerful generation capability.

4.3. Transfer to LAION-400M Dataset

Experiment Setting. We study the data compression on a more large-scale and challenging LAION-400M dataset [32]. We mostly follow the experiment settings in previous work [18]; the details can be found in the supplementary material. The only difference in training is that we make modifications to the pre-train dataset. In the BLIP paper, the pre-train dataset is a mixture of CC3M [35], CC12M [5], MSCOCO [20], VG [16], SBU [23], and LAION-400M [32] datasets. However, VG and SBU datasets potentially leak information in the downstream tasks, as SBU and VG datasets contain the information in the Flickr30K [28] and MSCOCO datasets, respectively. Towards a fair evaluation, the pre-train dataset in our experiment only contains CC3M, CC12M, and LAION-400M.

Downstream Tasks. Similarly, we consider two classical tasks in a zero-shot manner: image-text retrieval and image captioning.

Tab. 4 demonstrates the main result of image-text retrieval. Compared with the full-size datasets, we reduce the total training samples by $\sim 85\%$ and demonstrate significant improvements. For instance, we improve text recall@1 from 54.7% to 56.7% and image recall@1 from 41.5% to 42.6% on the MSCOCO dataset. It suggests that a large number of misaligned samples in the LAION-400M dataset seriously hurt the performance. We observe that

the performance between BLIP Score and CLIP Score is similar, for instance, 80.0% and 80.4% in text recall@1 on the Flickr30K dataset. However, it is noteworthy that our method achieves a $\sim 2.4\%$ improvement over BLIP-Score and CLIP-Score with the same volume. Integration with human knowledge brings the model an efficient and strong capability of fine-grained understanding.

Tab. 5 presents the main result of image captioning. We combine the compression of the LAION-400M dataset with the CC3M dataset and CC12M dataset from 130M to 15.5M. Compared with the full-size dataset, we reduce the total training samples by $\sim 90\%$ and achieve prominent performance improvements, for instance on MSCOCO dataset, from 9.1% to 19.8% on BLEU@4, 46.7% to 68.3% on CIDEr, 14.0% to 19.9% on METEOR, and 10.3% to 14.6% on SPICE. Compared with other filtering methods under the same volume, we outperform BLIP Score by +10.9% on CIDEr and +1.8% on SPICE validating on the Nocaps test set. The gap extends to +16.5% and +2.2% compared with CLIP Score. It indicates that less but high-quality image-text data is much more effective than cumbersome but noisy data.

4.4. Ablation Studies

Dataset Efficiency. We study the data compression under various compression ratios. The main results are demonstrated in Fig. 7. Our method consistently achieves significant improvements over other filtering baselines, demonstrating its good generalizability. It is noteworthy that the performance of our method degrades less than other methods with the compression of the training dataset. Compressing the dataset from 50% to 80%, our method observes a

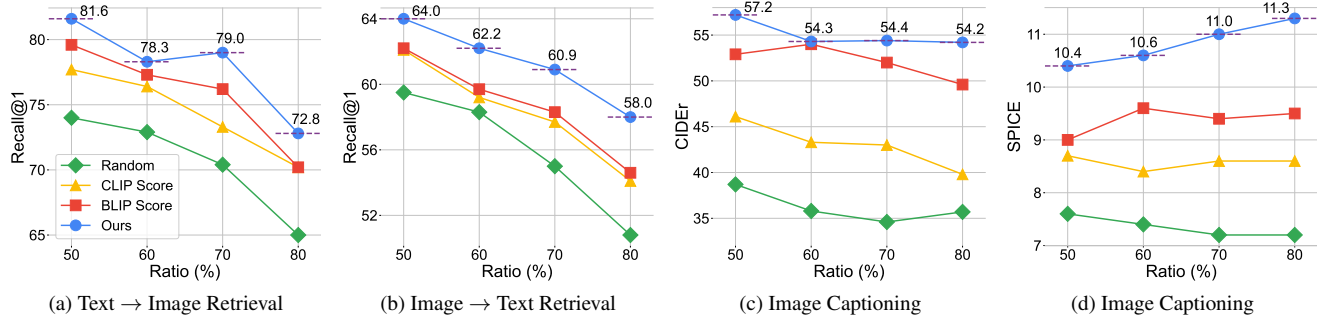


Figure 7. We set the compression ratio for CC12M dataset [5] to 50%, 60%, 70%, and 80%, respectively. The BLIP models with ViT-B/16 architecture are trained on compressed datasets and evaluated on zero-shot image-text retrieval on Flickr30K dataset [28] and zero-shot image captioning on Nocaps dataset [1].

Dataset	Method	#Samples	ImNet-1K Accuracy	ImNet-A Accuracy	ImNet-V2 Accuracy	Flickr30K					
						IR@1	IR@5	IR@10	TR@1	TR@5	TR@10
CC3M	-	2.82M	16.0	3.6	13.2	27.4	54.7	65.2	19.0	40.4	50.8
	Random	1.41M	13.7	3.5	11.2	24.2	50.2	62.1	16.8	37.6	45.9
	CLIP Score	1.41M	14.1	3.0	12.1	23.4	44.8	57.0	16.6	36.2	47.0
	BLIP Score	1.41M	15.6	2.9	12.9	28.9	54.9	66.8	19.6	41.6	52.4
	Ours	1.41M	15.0	4.1	13.0	31.0	57.0	67.9	21.0	44.0	55.2

Table 6. Zero-shot image classification results on ImageNet of different distributions and image-text retrieval results on Flickr30K [27] datasets on CLIP model of ViT-B/16. Here we adopt ImageNet-1K [8], ImageNet-A [10], and ImageNet-V2 [30].

decrease in performance of 3%, however, the decrease of BLIP Score is 4.4% in Fig. 7c. Moreover, our method gains improvements both in performance and efficiency. When the volume decreases from 50% to 20%, we observe an increase from 10.4 to 11.3 in Fig. 7d. This suggests that filtering misaligned samples directly brings out gains in the capability to align image and text features in both a fine-grained manner and a comprehensive manner.

Model Architecture. We generalize our method to another vision-language model CLIP [29] of ViT-B/16 [9]. Tab. 6 demonstrates the experiment results. Our method with the 50% dataset outperforms the full-size dataset on the retrieval task. For instance, we observe an increase in performance from 27.4% to 31.0% in IR@1 and from 19.0% to 21.0% in TR@1. For the classification task, our method demonstrates a good performance on ImageNet-A and ImageNet-V2 with +0.5% increase and slightly -0.2% gap, showing the generalization to different distributions. All results suggest the scalability of our method to different model architectures.

5. Conclusion

In this paper, we delve deep into image-text data. We present COCO-HF, an image-text dataset with human knowledge for alignment, and reveal that human knowledge enhances both data efficiency and visual-textual alignment. Scaling up to different datasets, we identify that our method shows significant performance on large-scale and

noisy datasets. Scaling to various downstream tasks, we discover that leveraging less but high-quality data leads to a greater abundance of fine-grained knowledge and is more suitable for captioning tasks. These findings underscore the potential of human knowledge in efficiency and alignment. Our findings can significantly enable faster training with better results. We hope that our work sheds light on the data-centric and human-centric field in the vision-language community and engages more and deeper exploration.

Acknowledgment

This work is partially supported by TPU Research Cloud (TRC) program and Google Cloud Research Credits program.

Supplementary Material

A. Training Details

Reward Model. We use ViT-L/16 BLIP model [18] to extract and fuse image and text embeddings and train an MLP using fused embedding as input to generate a scalar as reward score. Specifically, we use five-layer MLPs with 768, 1024, 128, 64, and 16 hidden dimensions each. We use the Dropout function between the first four layers with the 0.2, 0.2, and 0.1 ratios each. We freeze the pre-trained BLIP backbone and only train the MLP layers. We update the reward model using AdamW [14] optimizer with $\beta_1 = 0.9$, $\beta_2 = 0.999$, $\epsilon = 1e - 8$. The learning rate is set to $1e - 5$.

The model is trained on 2 NVIDIA 80GB A100 GPUs, with a per-GPU batch size of 32, resulting in a total batch size of 64. It is trained for a total of 20,000 updates.

BLIP. We train the ViT-B/16 BLIP model with a batch size of 2880 and ViT-L/16 BLIP model with a batch size of 2400 both for 20 epochs. We update models with AdamW [14] optimizer with $\beta_1 = 0.9$, $\beta_2 = 0.999$, $\epsilon = 1e-8$ and weight decay 0.05. The learning rate is warmed-up to $3e-4$ for ViT-B/16 and $2e-4$ for ViT-L/16 and decayed linearly with a rate of 0.85.

B. Additional Experiments

Ratio	Random	CLIP Score	BLIP Score	Ours
50%	74.0	77.7	79.6	81.6
60%	72.9	76.4	77.3	78.3
70%	70.4	73.3	76.2	79.0
80%	65.0	70.2	70.2	72.8

(a) Text Recall@1 on Flickr30K dataset.

Ratio	Random	CLIP Score	BLIP Score	Ours
50%	59.5	62.1	62.2	64.0
60%	58.3	59.2	59.7	62.2
70%	55.0	57.7	58.3	60.9
80%	50.8	54.1	54.6	58.0

(b) Image Recall@1 on Flickr30K dataset.

Ratio	Random	CLIP Score	BLIP Score	Ours
50%	38.7	46.1	52.9	57.2
60%	35.8	43.3	54.0	54.3
70%	34.6	43.0	54.0	54.3
80%	35.7	39.8	49.6	54.2

(c) CIDEr on Nocaps dataset.

Ratio	Random	CLIP Score	BLIP Score	Ours
50%	7.6	8.7	9.0	10.4
60%	7.4	8.4	9.6	10.6
70%	7.2	8.6	9.4	11.0
80%	7.2	8.6	9.5	11.3

(d) SPICE on Nocaps dataset.

Table 7. Zero-shot image-retrieval task on Flickr30K dataset [27] and image-captioning task on Nocaps dataset [1] with different compression ratio on BLIP ViT-B/16 model [18] and CC12M dataset [5].

B.1. Ablation Study on Vision Backbone

We conduct experiments on the vision backbone of BLIP model to ViT-L/16. The main results are demonstrated in Tab. 10 and Tab. 11. When reducing the dataset to 50%,

Our method outperforms the full-size dataset by over 2% on text recall@1, nearly 1% on image recall@1, over 15% on CIDEr, and over 3% on SPICE. Compared with other filtering methods with the same amount of data, we demonstrate significant advantages in both image-text retrieval and image captioning tasks. For instance, we improve text recall@1 from 79.3 to 83.5 on the Flickr30K dataset and from 52.3 to 56.8 on the MSCOCO dataset compared with the CLIP Score. It suggests that our method is flexible to various vision backbones.

B.2. Ablation Study on Data Efficiency

We provide detailed experiment results on different compression ratios in Section 4.4 in the main paper. The main results are demonstrated in Tab. 7. Our method outperforms other filtering methods consistently under different compression ratios. For instance, our method improves by an average of +1.9% on text recall@1, +2.6% on image recall@1, +2.4% on CIDEr, and +1.5% on SPICE over BLIP Score. It is noteworthy CIDEr performs a minor decline with the decrease of data volume and SPICE even improves +1% while the training samples reduce 30%. The outperforming results show that our method is successfully generalized to datasets with different scales.

B.3. Comparison with BLIP Model

We follow the setting in [18] to demonstrate the effectiveness of our method. The pre-training dataset consists of CC3M [35], CC12M [5], COCO [20], SBU [23], VG [16], and LAION-400M [32] datasets.

The main results are shown in Tab. 8 and Tab. 9. The performance of our method becomes slightly worse than BLIP-Capfilt on image-text retrieval tasks. Firstly, it can be attributed to the increase in data since VG and SBU contain part of the samples from Flickr30K and MSCOCO datasets, which is not fair to some extent. However, our method outperforms VG and SBU without VG and SBU datasets (Table. 4, main paper), which still demonstrates the superiority of our method to some extent. Secondly, BLIP-Capfilt rewrites the textual captions of misaligned image-text pairs, while we only filter the misaligned pairs. The rewriting enhances the data quality and provides more useful information for fine-grained understanding.

As shown in Tab. 9, although BLIP-CapFilt utilizes caption rewriting and more than $7\times$ data, our method performs significant advantages on image captioning tasks. We demonstrate improvements of 9.2% in CIDEr, 2.8% in BLEU@4, 1.4% in METEOR, and 1.9% in SPICE on the MSCOCO dataset compared to BLIP-CapFilt. Similarly, we outperform BLIP-CapFilt by an average of 0.7% in CIDEr and 0.5% in SPICE on the Nocaps dataset. The caption rewriting model of BLIP-CapFilt is trained on the MSCOCO dataset. The captions in the MSCOCO dataset

Dataset	Method	#Samples	Retrieval (COCO)		Retrieval (Flickr30K)		Caption (COCO)		Caption (Nocaps)	
			TR@1	IR@1	TR@1	IR@1	CIDEr	SPICE	CIDEr	SPICE
COCO+VG+CC +SBU+LAION	BLIP-CapFilt	129M	72.2	57.7	89.0	79.6	95.2	17.7	74.4	10.7
	Ours	17.6M	68.9	52.9	89.4	72.2	104.4	19.0	74.8	11.1

Table 8. Zero-shot evaluation of BLIP ViT-B/16 models trained with [18] and our method on downstream tasks. BLIP-CapFilt means bootstrapping with caption rewrite and filtering with ViT-L/16 models proposed in [18]. Note that the models are not fine-tuned before evaluation.

Dataset	Method	#Samples	MSCOCO				NoCaps			
			BLEU@4	CIDEr	METEOR	SPICE	Valid		Test	
							CIDEr	SPICE	CIDEr	SPICE
COCO+VG+CC +SBU+LAION	BLIP-CapFilt	129M	28.2	95.2	23.2	17.1	74.4	10.7	72.2	10.5
	Ours	17.6M	31.0	104.4	24.6	19.0	74.8	11.1	73.3	11.1

Table 9. Zero-shot image captioning results on MSCOCO [20] and NoCaps [1] datasets. Note that the models are not finetuned with CIDEr optimization on MSCOCO dataset.

Dataset	Method	#Samples	Text → Image						Image → Text					
			Flickr30K			MSCOCO			Flickr30K			MSCOCO		
			R@1	R@5	R@10	R@1	R@5	R@10	R@1	R@5	R@10	R@1	R@5	R@10
CC12M	-	10.4M	81.1	95.6	98.0	54.6	79.7	87.2	68.4	89.1	93.0	40.9	67.1	76.8
	CLIP Score	5.20M	79.3	95.9	97.2	52.3	77.7	85.4	64.7	85.5	90.6	38.7	64.7	74.1
	BLIP Score	5.20M	81.5	95.4	97.7	54.8	80.4	87.4	68.1	89.0	93.0	40.8	68.1	77.5
	Ours	5.20M	83.5	96.4	98.6	56.8	80.6	87.8	66.9	88.9	93.4	41.7	67.7	77.0

Table 10. Zero-shot image-text retrieval results on Flickr30K [27] and MSCOCO [20] datasets.

Dataset	Method	#Samples	MSCOCO				NoCaps			
			BLEU@4	CIDEr	METEOR	SPICE	Valid		Test	
							CIDEr	SPICE	CIDEr	SPICE
CC12M	-	10.4M	13.1	52.2	15.8	11.6	43.8	8.1	41.8	8.0
	CLIP Score	5.20M	15.3	55.4	17.5	12.8	49.4	8.9	46.1	8.8
	BLIP Score	5.20M	19.0	66.6	19.4	14.6	56.2	9.4	54.8	9.5
	Ours	5.20M	20.3	68.2	20.7	15.4	63.8	11.0	60.5	11.0

Table 11. Zero-shot image captioning results on MSCOCO [20] and NoCaps [1] datasets. Note that the models are not finetuned with CIDEr optimization on MSCOCO dataset.

are plain and simple. Admittedly, it perhaps contains more visual objects and simple descriptions which boosts retrieval tasks, however, it lacks vivid details which are crucial to captioning tasks and are meticulously formulated in our method.

C. Visualization of COCO-HF Dataset

We visualize the image-text pairs in the COCO-HF dataset, as shown in Fig. 8. Furthermore, we make annotations on the textual captions following the proposed criteria for human-preference annotations in Section 3.1 of the main paper. It demonstrates that the textual captions in the dataset differ in completeness, vividity, and description of context.



A man in a yellow vest standing next to a white truck with a hose attached to a fire hydrant.

a man in a reflective vest standing next to a fire hydrant and a truck

a man standing next to a fire hydrant



There is a man sitting on the couch next to a woman but he has three neck ties on.

a man wearing a tie sitting next to a woman wearing glasses sitting on a couch

A man on a couch who is wearing several ties.

a man and woman sitting on a couch.



a baseball player swings his bat at a pitch while the catcher and umpire behind him play a game of baseball on the field.

a baseball batter in red and white on a baseball field



a small dog standing in a green field of grass next to a blue and white soccer ball

A pug dog with its paw on a soccer ball on field.

a pug is playing with a soccer ball in the grass

A small dog is playing with a soccer ball.

Figure 8. Visualization of image-text pair in COCO-HF dataset. We make annotations on each caption based on the criteria mentioned in Section 3.1 in the main paper. We used different colors to demonstrate visual objects, vivid details, and context.

References

- [1] Harsh Agrawal, Peter Anderson, Karan Desai, Yufei Wang, Xinlei Chen, Rishabh Jain, Mark Johnson, Dhruv Batra, Devi Parikh, and Stefan Lee. nocaps: novel object captioning at scale. In *ICCV*, pages 8947–8956, 2019. 2, 6, 8, 9, 10
- [2] Jean-Baptiste Alayrac, Jeff Donahue, Pauline Luc, Antoine Miech, Iain Barr, Yana Hasson, Karel Lenc, Arthur Mensch, Katherine Millican, Malcolm Reynolds, Roman Ring, Eliza Rutherford, Serkan Cabi, Tengda Han, Zhitao Gong, Sina Samangooei, Marianne Monteiro, Jacob L. Menick, Sebastian Borgeaud, Andy Brock, Aida Nematzadeh, Sahand Sharifzadeh, Mikolaj Binkowski, Ricardo Barreira, Oriol Vinyals, Andrew Zisserman, and Karén Simonyan. Flamingo: a visual language model for few-shot learning. In *NeurIPS*, 2022. 1, 2
- [3] Dzmitry Bahdanau, Philemon Brakel, Kelvin Xu, Anirudh Goyal, Ryan Lowe, Joelle Pineau, Aaron C. Courville, and Yoshua Bengio. An actor-critic algorithm for sequence prediction. In *ICLR*, 2017. 2
- [4] Ralph Allan Bradley and Milton E Terry. Rank analysis of incomplete block designs: I. the method of paired comparisons. *abs/1707.06347:39(3/4):324–345*, 1952. 4
- [5] Soravit Changpinyo, Piyush Sharma, Nan Ding, and Radu Soricut. Conceptual 12m: Pushing web-scale image-text pre-training to recognize long-tail visual concepts. In *CVPR*, pages 3558–3568, 2021. 1, 2, 5, 7, 8, 9
- [6] Paul F. Christiano, Jan Leike, Tom B. Brown, Miljan Martic, Shane Legg, and Dario Amodei. Deep reinforcement learning from human preferences. In *NIPS*, pages 4299–4307, 2017. 2
- [7] Wenliang Dai, Junnan Li, Dongxu Li, Anthony Meng Huat Tiong, Junqi Zhao, Weisheng Wang, Boyang Li, Pascale Fung, and Steven C. H. Hoi. Instructblip: Towards general-purpose vision-language models with instruction tuning. *CoRR*, abs/2305.06500, 2023. 3
- [8] Jia Deng, Wei Dong, Richard Socher, Li-Jia Li, Kai Li, and Li Fei-Fei. Imagenet: A large-scale hierarchical image database. In *CVPR*, pages 248–255, 2009. 6, 8
- [9] Alexey Dosovitskiy, Lucas Beyer, Alexander Kolesnikov, Dirk Weissenborn, Xiaohua Zhai, Thomas Unterthiner, Mostafa Dehghani, Matthias Minderer, Georg Heigold, Sylvain Gelly, Jakob Uszkoreit, and Neil Houlsby. An image is worth 16x16 words: Transformers for image recognition at scale. *CoRR*, abs/2010.11929, 2020. 5, 8
- [10] Dan Hendrycks, Kevin Zhao, Steven Basart, Jacob Steinhardt, and Dawn Song. Natural adversarial examples. In *CVPR*, pages 15262–15271, 2021. 6, 8
- [11] Chao Jia, Yinfei Yang, Ye Xia, Yi-Ting Chen, Zarana Parekh, Hieu Pham, Quoc V. Le, Yun-Hsuan Sung, Zhen Li, and Tom Duerig. Scaling up visual and vision-language representation learning with noisy text supervision. In *ICML*, pages 4904–4916, 2021. 1, 2
- [12] Andrej Karpathy and Li Fei-Fei. Deep visual-semantic alignments for generating image descriptions. *IEEE Trans. Pattern Anal. Mach. Intell.*, 39(4):664–676, 2017. 5, 6
- [13] Wonjae Kim, Bokyung Son, and Ildoo Kim. Vilt: Vision-and-language transformer without convolution or region supervision. In *ICML*, pages 5583–5594, 2021. 5
- [14] Diederik P. Kingma and Jimmy Ba. Adam: A method for stochastic optimization. In *ICLR*, 2015. 5, 8, 9
- [15] Julia Kreutzer, Shahram Khadivi, Evgeny Matusov, and Stefan Riezler. Can neural machine translation be improved with user feedback? In *NACCL-HIT*, pages 92–105, 2018. 2
- [16] Ranjay Krishna, Yuke Zhu, Oliver Groth, Justin Johnson, Kenji Hata, Joshua Kravitz, Stephanie Chen, Yannis Kalantidis, Li-Jia Li, David A. Shamma, Michael S. Bernstein, and Li Fei-Fei. Visual genome: Connecting language and vision using crowdsourced dense image annotations. *Int. J. Comput. Vis.*, 123(1):32–73, 2017. 7, 9
- [17] Kimin Lee, Hao Liu, Moonkyung Ryu, Olivia Watkins, Yuqing Du, Craig Boutilier, Pieter Abbeel, Mohammad Ghavamzadeh, and Shixiang Shane Gu. Aligning text-to-image models using human feedback. *CoRR*, abs/2302.12192, 2023. 2
- [18] Junnan Li, Dongxu Li, Caiming Xiong, and Steven C. H. Hoi. BLIP: bootstrapping language-image pre-training for unified vision-language understanding and generation. In *ICML*, pages 12888–12900, 2022. 3, 4, 5, 7, 8, 9, 10
- [19] Junnan Li, Dongxu Li, Silvio Savarese, and Steven C. H. Hoi. BLIP-2: bootstrapping language-image pre-training with frozen image encoders and large language models. In *ICML*, pages 19730–19742, 2023. 3
- [20] Tsung-Yi Lin, Michael Maire, Serge J. Belongie, James Hays, Pietro Perona, Deva Ramanan, Piotr Dollár, and C. Lawrence Zitnick. Microsoft COCO: common objects in context. In *ECCV*, pages 740–755, 2014. 1, 3, 4, 5, 6, 7, 9, 10
- [21] James MacGlashan, Mark K. Ho, Robert Tyler Loftin, Bei Peng, Guan Wang, David L. Roberts, Matthew E. Taylor, and Michael L. Littman. Interactive learning from policy-dependent human feedback. In *ICML*, pages 2285–2294, 2017. 2
- [22] Reiichiro Nakano, Jacob Hilton, Suchir Balaji, Jeff Wu, Long Ouyang, Christina Kim, Christopher Hesse, Shantanu Jain, Vineet Kosaraju, William Saunders, Xu Jiang, Karl Cobbe, Tyna Eloundou, Gretchen Krueger, Kevin Button, Matthew Knight, Benjamin Chess, and John Schulman. Webgpt: Browser-assisted question-answering with human feedback. *CoRR*, abs/2112.09332, 2021. 2
- [23] Vicente Ordonez, Girish Kulkarni, and Tamara L. Berg. Im2text: Describing images using 1 million captioned photographs. In *NIPS*, pages 1143–1151, 2011. 7, 9
- [24] Mayu Otani, Riku Togashi, Yu Sawai, Ryosuke Ishigami, Yuta Nakashima, Esa Rahtu, Janne Heikkilä, and Shin’ichi Satoh. Toward verifiable and reproducible human evaluation for text-to-image generation. In *CVPR*, pages 14277–14286, 2023. 2
- [25] Long Ouyang, Jeffrey Wu, Xu Jiang, Diogo Almeida, Carroll L. Wainwright, Pamela Mishkin, Chong Zhang, Sandhini Agarwal, Katarina Slama, Alex Ray, John Schulman, Jacob Hilton, Fraser Kelton, Luke Miller, Maddie Simens, Amanda Askell, Peter Welinder, Paul F. Christiano, Jan Leike, and

- Ryan Lowe. Training language models to follow instructions with human feedback. In *NeurIPS*, 2022. 2, 3, 4
- [26] Hieu Pham, Zihang Dai, Golnaz Ghiasi, Kenji Kawaguchi, Hanxiao Liu, Adams Wei Yu, Jiahui Yu, Yi-Ting Chen, Minh-Thang Luong, Yonghui Wu, Mingxing Tan, and Quoc V. Le. Combined scaling for zero-shot transfer learning. *Neurocomputing*, 555:126658, 2023. 1
- [27] Bryan A. Plummer, Liwei Wang, Chris M. Cervantes, Juan C. Caicedo, Julia Hockenmaier, and Svetlana Lazebnik. Flickr30k entities: Collecting region-to-phrase correspondences for richer image-to-sentence models. In *ICCV*, pages 2641–2649, 2015. 5, 6, 8, 9, 10
- [28] Bryan A. Plummer, Liwei Wang, Chris M. Cervantes, Juan C. Caicedo, Julia Hockenmaier, and Svetlana Lazebnik. Flickr30k entities: Collecting region-to-phrase correspondences for richer image-to-sentence models. In *ICCV*, pages 2641–2649, 2015. 2, 7, 8
- [29] Alec Radford, Jong Wook Kim, Chris Hallacy, Aditya Ramesh, Gabriel Goh, Sandhini Agarwal, Girish Sastry, Amanda Askell, Pamela Mishkin, Jack Clark, Gretchen Krueger, and Ilya Sutskever. Learning transferable visual models from natural language supervision. In *ICML*, pages 8748–8763, 2021. 1, 2, 5, 6, 8
- [30] Benjamin Recht, Rebecca Roelofs, Ludwig Schmidt, and Vaishal Shankar. Do imagenet classifiers generalize to imagenet? In *ICML*, pages 5389–5400, 2019. 8
- [31] Nataniel Ruiz, Yuanzhen Li, Varun Jampani, Yael Pritch, Michael Rubinstein, and Kfir Aberman. Dreambooth: Fine tuning text-to-image diffusion models for subject-driven generation. In *CVPR*, pages 22500–22510, 2023. 2
- [32] Christoph Schuhmann, Richard Vencu, Romain Beaumont, Robert Kaczmarczyk, Clayton Mullis, Aarush Katta, Theo Coombes, Jenia Jitsev, and Aran Komatsuzaki. LAION-400M: open dataset of clip-filtered 400 million image-text pairs. *CoRR*, abs/2111.02114, 2021. 1, 2, 5, 7, 9
- [33] Christoph Schuhmann, Romain Beaumont, Richard Vencu, Cade Gordon, Ross Wightman, Mehdi Cherti, Theo Coombes, Aarush Katta, Clayton Mullis, Mitchell Wortsman, Patrick Schramowski, Srivatsa Kundurthy, Katherine Crowson, Ludwig Schmidt, Robert Kaczmarczyk, and Jenia Jitsev. LAION-5B: an open large-scale dataset for training next generation image-text models. In *NeurIPS*, 2022. 1
- [34] John Schulman, Filip Wolski, Prafulla Dhariwal, Alec Radford, and Oleg Klimov. Proximal policy optimization algorithms. *CoRR*, abs/1707.06347, 2017. 2
- [35] Piyush Sharma, Nan Ding, Sebastian Goodman, and Radu Soricut. Conceptual captions: A cleaned, hypernymed, image alt-text dataset for automatic image captioning. In *ACL*, pages 2556–2565, 2018. 1, 2, 5, 7, 9
- [36] Nisan Stiennon, Long Ouyang, Jeffrey Wu, Daniel M. Ziegler, Ryan Lowe, Chelsea Voss, Alec Radford, Dario Amodei, and Paul F. Christiano. Learning to summarize with human feedback. In *NIPS*, 2020. 2
- [37] Bart Thomee, David A. Shamma, Gerald Friedland, Benjamin Elizalde, Karl Ni, Douglas Poland, Damian Borth, and Li-Jia Li. YFCC100M: the new data in multimedia research. *Commun. ACM*, 59(2):64–73, 2016. 1, 2
- [38] Alex Jinpeng Wang, Kevin Qinghong Lin, David Junhao Zhang, Stan Weixian Lei, and Mike Zheng Shou. Too large; data reduction for vision-language pre-training. *CoRR*, abs/2305.20087, 2023. 1, 2
- [39] Xiaoshi Wu, Keqiang Sun, Feng Zhu, Rui Zhao, and Hongsheng Li. Better aligning text-to-image models with human preference. *CoRR*, abs/2303.14420, 2023. 2
- [40] Hu Xu, Saining Xie, Po-Yao Huang, Licheng Yu, Russell Howes, Gargi Ghosh, Luke Zettlemoyer, and Christoph Feichtenhofer. Cit: Curation in training for effective vision-language data. *CoRR*, abs/2301.02241, 2023. 1, 2
- [41] Jiazheng Xu, Xiao Liu, Yuchen Wu, Yuxuan Tong, Qinkai Li, Ming Ding, Jie Tang, and Yuxiao Dong. Imagereward: Learning and evaluating human preferences for text-to-image generation. *CoRR*, abs/2304.05977, 2023. 2, 4
- [42] Pengchuan Zhang, Xiujun Li, Xiaowei Hu, Jianwei Yang, Lei Zhang, Lijuan Wang, Yejin Choi, and Jianfeng Gao. Vinvl: Revisiting visual representations in vision-language models. In *CVPR*, pages 5579–5588, 2021. 5
- [43] Shu Zhang, Xinyi Yang, Yihao Feng, Can Qin, Chia-Chih Chen, Ning Yu, Zeyuan Chen, Huan Wang, Silvio Savarese, Stefano Ermon, Caiming Xiong, and Ran Xu. HIVE: harnessing human feedback for instructional visual editing. *CoRR*, abs/2303.09618, 2023. 2
- [44] Wangchunshu Zhou and Ke Xu. Learning to compare for better training and evaluation of open domain natural language generation models. In *AAAI*, pages 9717–9724, 2020. 2